Available online at www.sciencedirect.com
ScienceDirect
Journal of Environmental Sciences 2010, 22(4) 555–560
JOURNAL OF ENVIRONMENTAL SCIENCES
ISSN 1001-0742
CN 11-2629/X
www.jesc.ac.cn

In situ DRIFTS study of hygroscopic behavior of mineral aerosol

Qingxin Ma, Hong He*, Yongchun Liu

State Key Laboratory of Environmental Chemistry and Ecotoxicology, Research Center for Eco-Environmental Sciences, Chinese Academy of Sciences, Beijing 100085, China. E-mail: 5237027@rcees.ac.cn

Received 09 October 2009; revised 10 November 2009; accepted 19 November 2009

Abstract

In situ diffusion reflectance infrared Fourier transform spectroscopy was used to study the water adsorption on mineral oxides (SiO_2, α-Al_2O_3, MgO, Fe_2O_3, TiO_2). The results showed that all the water adsorption isotherms were well fitted with the Brunauer-Emmett-Teller (BET)-III type equation, with the calculated monolayers occurring at 24%–30% relative humidity. It showed that about 1–5 layers of water adsorbed on oxides surfaces in ambient relative humidity (20%–90%). The measured deliquescence relative humidity of NaCl was (74 ± 1)%, which demonstrated that DRIFTS is a useful method for the study the hygroscopic behavior of mineral dust. In addition, the limits of DRIFTS were also discussed.

Key words: DRIFTS; mineral oxides; water adsorption; hygroscopicity

DOI: 10.1016/S1001-0742(09)60145-5

Introduction

Mineral aerosols are produced from wind-blown soils and represent an important component of the earth's atmosphere. It is currently estimated that between 1000 and 3000 Tg of mineral aerosols are emitted annually into the atmosphere (d'Almeida, 1987; Tegen and Fung, 1994). Mineral aerosols play an important role in the global climate change by absorbing and scattering solar radiation as well as acting as cloud condensation nucleus, which is the major uncertainty for future climate change prediction (IPCC, 2007). Modeling, field observations and laboratory study suggest that mineral aerosol could act as a reactive surface with trace atmospheric gases, thus, influencing the trace atmospheric gas budget through heterogeneous reactions (Zhang et al., 1994; Dentener et al., 1996; Usher et al., 2003), and aerosol water content has been reported to affect the uptake rate of reactive gases (Liu et al., 2009). Therefore, measurements of hygroscopic growth and associated water content are necessary to understand the radiative and chemical effects of tropospheric aerosol species.

Because it is ease for sample preparation, and it is able to analyze nontransparent materials as well as to make *in situ* measurement at elevated temperature, *in situ* diffusion reflectance infrared Fourier transform spectroscopy (DRIFTS) has been demonstrated as a useful technology for surface science and heterogeneous reactions analysis (Fuller and Griffiths, 1978; Armaroli et al., 2004; He et al., 2005). However, the utilization of *in situ* DRIFTS for the hygroscopic behavior of mineral dusts was little reported. Gustafsson et al. (2005) used the DRIFTS to study the water adsorption on calcite and Arizona test dust, and it demonstrated that DRIFTS results have a good consistency with other methods. In this study, we applied the DRIFTS to study water adsorption on mineral oxides. The influences of heterogeneous reactions with NO_2 on the hygroscopic behavior change were also investigated. These results will improve our understanding of the relation between atmospheric aging processes and hygroscopicity of mineral aerosols.

1 Experimental section

The reaction system is depicted in Fig. 1. *In situ* DRIFTS spectra were recorded on a Nicolet 6700 (Thermo Nicolet Instrument Corporation, USA) FT-IR, equipped with an *in situ* diffuse reflection chamber and a high-sensitivity mercury cadmium telluride (MCT) detector cooled by liquid N_2. The sample (about 11 mg) for the *in situ* DRIFTS studies was finely ground and placed into a ceramic crucible in the *in situ* chamber. The total flow rate was 100 mL/min in all flow systems, and the volume of the closed system was about 30 mL. The samples were heated in N_2 atmosphere at 100°C to remove surface species for 3 hr. The reference spectrum was measured after the pretreated sample was cooled to 30°C. Nitrated oxides were *in situ* prepared by the reactions of the fresh sample exposed to NO (200×10^{-6}, *V/V*) with stimulated air (79% N_2 + 21% O_2) at 30°C for 2 hr in the *in situ* cell. When the spectrum showed no change, the introduction of NO

* Corresponding author. E-mail: honghe@rcees.ac.cn

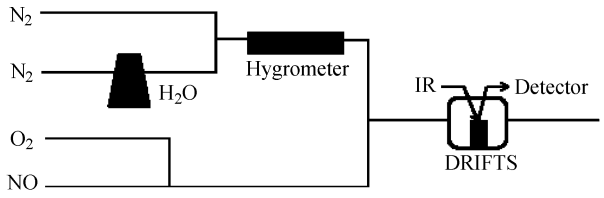

Fig. 1 Schematic of the reaction system.

and O_2 were ceased and the nitrated sample was purged by N_2 for 1 hr to remove the gaseous NO and NO_2 in the flow system. The infrared spectra were collected and analyzed using a data acquisition computer with OMNIC 6.0 software (Nicolet Corp., USA). All spectra reported here were recorded at a resolution of 4 cm^{-1} for 100 scans and were converted to Kubelka-Munk form directly. The low frequency cutoff below 1000 cm^{-1} is owing to strong lattice oxide absorptions. The relative humidity (RH) in the reaction system, which was recorded by a moisture meter, was controlled by changing the mixture ratio of dry N_2 and humid N_2.

Silicon dioxide and titanium dioxide were purchased from Degussa (Germany), while NaCl, Fe_2O_3, and MgO were purchased from Beijng Chemical Reagents Company (China). α-Al_2O_3 was produced by calcinations of AlOOH (Shangdong Alumina, China) at 1200°C for 12 hr. NO (1.01% N_2, Huayuan, China) was used as received.

2 Results and discussion

2.1 Adsorption of water on NaCl

Adsorption of water on NaCl was first conducted. It is a relatively simple system to study because it does not form crystalline hydrates and there is no spectral interference from the salt itself. As shown in Fig. 2a, several bands increased simultaneously with the increase of relative humidity, which are attribute to the vibration of water according to literature (Goodman et al., 2001; Al-Abadleh and Grassian, 2003; Gustafsson et al., 2005). The main absorption features observed in the spectra were 3420 cm^{-1} with a shoulder at 3240 cm^{-1}, 2100 cm^{-1} and 1640 cm^{-1}. The peak 1640 cm^{-1} is attributed to the bending mode of water, δ_{H_2O}. For liquid water, the broad feature centered at 2100 cm^{-1} is assigned to an association band (ν_a) which is a combination of the bending (δ), libration (ν_L), and hindered translation (ν_T), modes (Al-Abadleh and Grassian, 2003). The peak in the region of 2600–3800 cm^{-1} is a combination of OH vibrational modes: symmetric stretch around 3420 cm^{-1} and asymmetric stretch around 3240 cm^{-1}. The absorbance of these modes is suitable to monitor water adsorption on the surfaces of the particles; therefore the integrated intensity of the O–H stretching region provides a measure of the amount of water on the surface (Goodman et al., 2001; Gustafsson et al., 2005).

The reflected radiation in DRIFTS is dependent on many factors, including particle dimension, packing density and homogeneity, etc. (Armaroli et al., 2004). In addition,

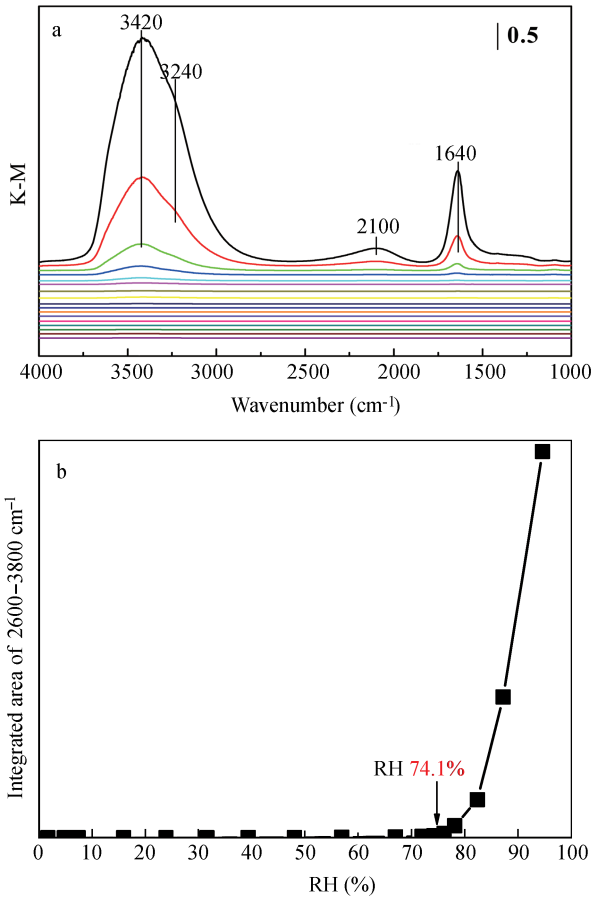

Fig. 2 DRIFTS spectra of water adsorption on NaCl at 30°C as a function of RH (%) (1.7, 4.8, 7.4, 15.9, 23.9, 31.6, 39.3, 48.0, 56.9, 67.0, 72.0, 74.2, 76.1, 78.1, 82.4, 87.2, 94.6) (a). Integration intensity of the bands of the region 2600–3800 cm^{-1} (b). RH: relative humidity.

unlike transmission FT-IR, DRIFTS shows no linear relation between band intensity and concentration. Gaining quantitative information from the spectra is non-trivial because the Beer-Lambert law used in transmittance is not applicable in this case. However, Kubelka-Munk theory can be applied to improve the linearity of the dependence of signal intensity upon concentration (Armaroli et al., 2004). The DRIFTS spectrum contains both reflection and absorption signals of incident flux on a particle. The absorption fraction is easily known from the Lambert-Beer law. The reflection fraction in the case of infinite thickness (2–3 mm) could be a similar expression to the absorption expression after applying the Kubelka-Munk function (Armaroli et al., 2004). Therefore, the Kubelka-Munk conversion leads to a linear relationship between concentration and reflected radiation intensity for DRIFTS spectra.

There was a relatively small increase in the observed integrated absorbance of the water absorption bands under the RH value of 74.2% (Fig. 2b). When the relative humidity exceeded this value, the integrated absorbance abruptly became quite intense and continued to grow in intensity with relative humidity increasing. This sharp increase in water content of the NaCl particles occurred at RH value (74 ± 1)%. This sharp transition marked the deliquescence relative humidity (DRH) of NaCl. This DRH of NaCl is

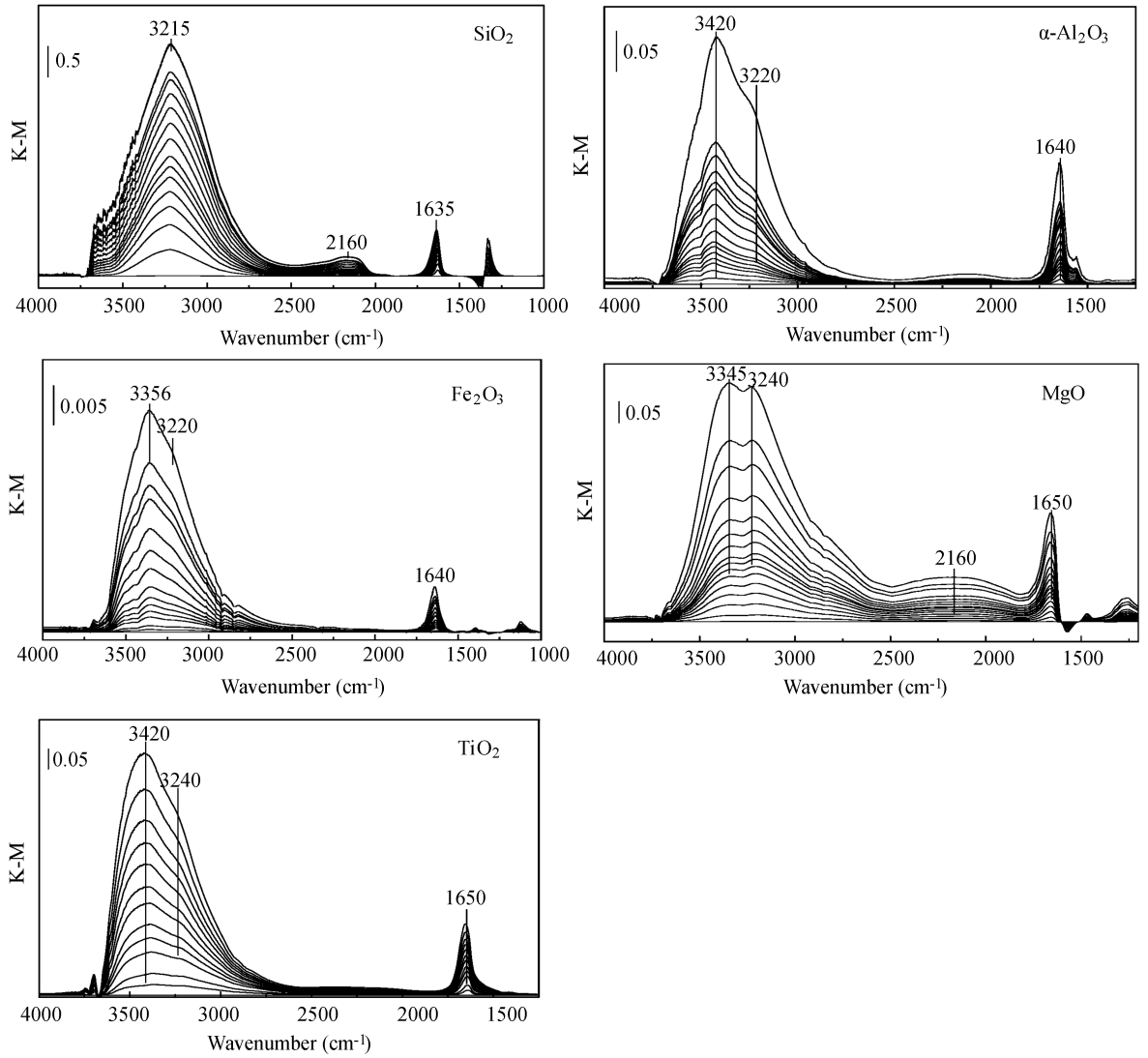

Fig. 3 DRIFTS spectra of water adsorption on SiO_2, α-Al_2O_3, MgO, Fe_2O_3, TiO_2 as a function of relative humidities (2%–96% RH) at 30°C.

in good agreement with other studies (Cziczo and Abbatt, 2000; Krueger et al., 2003).

2.2 Water adsorption on oxides

The DRIFTS spectra of water adsorption on SiO_2, α-Al_2O_3, MgO, Fe_2O_3, TiO_2 as a function of relative humidities are shown in Fig. 3. For all these oxides, several peaks were observed at 2600–3800 cm^{-1}, 2100–2200 cm^{-1}, and 1630–1650 cm^{-1}, which are similarly attributed to stretch mode, association mode and bending mode as mentioned above for water absorption on NaCl. Since the IR absorption of gas-phase water was also contributed to the region of 2600–3800 cm^{-1} and it can not be removed by reference subtraction in different RH, the absorption of gas-phase water was measured with a hydrophobic gold mirror as sample. The comparison of the integrated intensity of water adsorption in 2600–3800 cm^{-1} on SiO_2 and gold mirror are shown in Fig. 4. It suggests that contribution of gas-phase water IR absorption to the surface adsorbed absorption could be neglected.

Figure 5 shows the water adsorption isotherms obtained after applying the Kubelka-Munk function to the DRIFTS

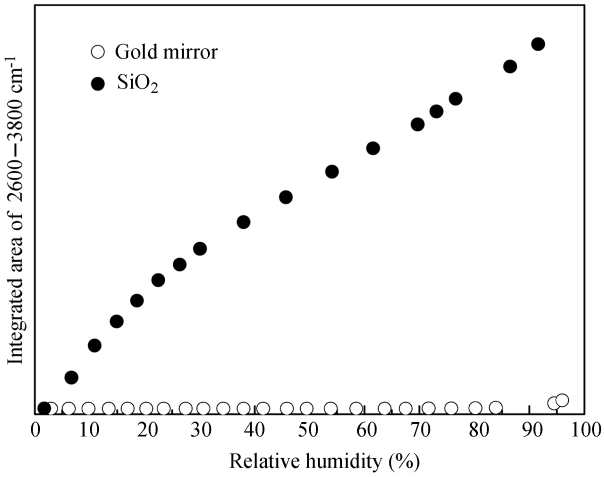

Fig. 4 Comparison of water adsorption isotherms on SiO_2 and gold mirror.

data. The isotherms exhibit a type III adsorption isotherm characteristic which indicates a low adsorption enthalpy in the contact layer. It could be fitted with three-parameters Brunauer-Emmett-Teller (BET) equation with the assump-

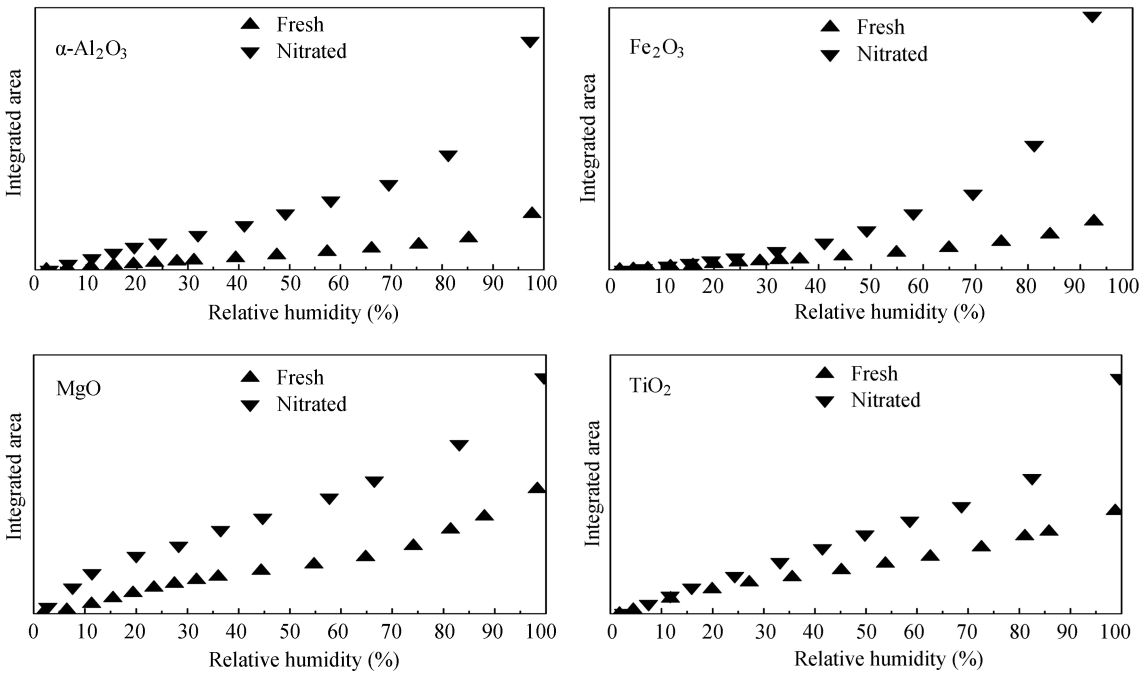

Fig. 5 Water adsorption isotherms of oxides and nitrated oxides at 30°C. The integrated region of OH was in the range of 2600–3800 cm^{-1}.

tion of limited adsorbed water layers ($n \neq \infty$) as following Eq. (1) (Brunauer et al., 1938, 1940):

$$V = \frac{V_m c \frac{P}{P_0}}{1-\frac{P}{P_0}} \times \frac{1-(n+1)(\frac{P}{P_0})^n + n(\frac{P}{P_0})^{n+1}}{1+(c-1)(\frac{P}{P_0}) - c(\frac{P}{P_0})^{n+1}} \quad (1)$$

where, V is the volume of gas adsorbed at equilibrium pressure P, V_m is the volume of gas necessary to cover the surface of the adsorbent with a complete monolayer, P is the equilibrium pressure of the adsorbing gas, and P_0 is the saturation vapor pressure of the adsorbing gas at that temperature. n is an adjustable parameter given as the maximum number of layers of the adsorbing gas and is related to the pore size and properties of adsorbent. As a result, multilayer formation of adsorbing gas is limited to n layers at large values of P/P_0. The parameter c is the temperature-dependent constant related to the enthalpies of adsorption of the first and higher layers through Eq. (2):

$$c = \exp(\frac{\Delta H_2^0 - \Delta H_1^0}{RT}) \quad (2)$$

where, ΔH_1^0 is the standard enthalpy of adsorption of the first layer, ΔH_2^0 is the standard enthalpy of adsorption on subsequent layers and is taken as the standard enthalpy of condensation, R is the gas constant, and T is the temperature in Kelvin.

A curve-fit software (CurveExpert 1.3) was used to fit the 3 parameter BET equation for the isotherms of oxides, and the parameters calculated are shown in Table 1. The fitting curves are shown in Fig. 6. The results show that the water monolayer adsorption on oxides occurred at 24%–30% RH. With the fitted value of integration intensity of monolayer, we can convert the adsorption integration

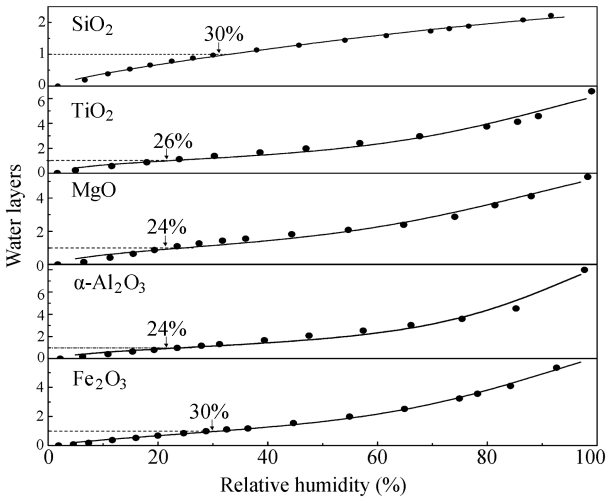

Fig. 6 Water adsorption isotherms of oxides (points) and fitting curves (lines) with III-parameters BET equation.

Table 1 Adsorption parameters for water uptake on oxide particles

Oxides	BET area (m^2/g)	M-RH (%)	n	c	E_{ad}	P/P_0
SiO_2	420	29	3.8	4.8	–47.95	1.8–92.6 (0.997)*
MgO	14.5	24	9.5	9.5	–49.67	1.8–98.3 (0.991)
TiO_2	12.7	26	6.2	5.5	–48.29	1.8–95.8 (0.997)
Fe_2O_3	2.7	30	11.3	4.68	–47.88	1.9–92.6 (0.998)
α-Al_2O_3	12	24	15.4	9.66	–49.71	2.2–97.7 (0.990)

* Data shown in parenthesis are correlation coefficient.
n: adjustable parameter; c: the temperature-dependent constant; M-RH: the relative humidity where monolayer adsorbed water is formed; $E_{ad} = \Delta H_1^0$.

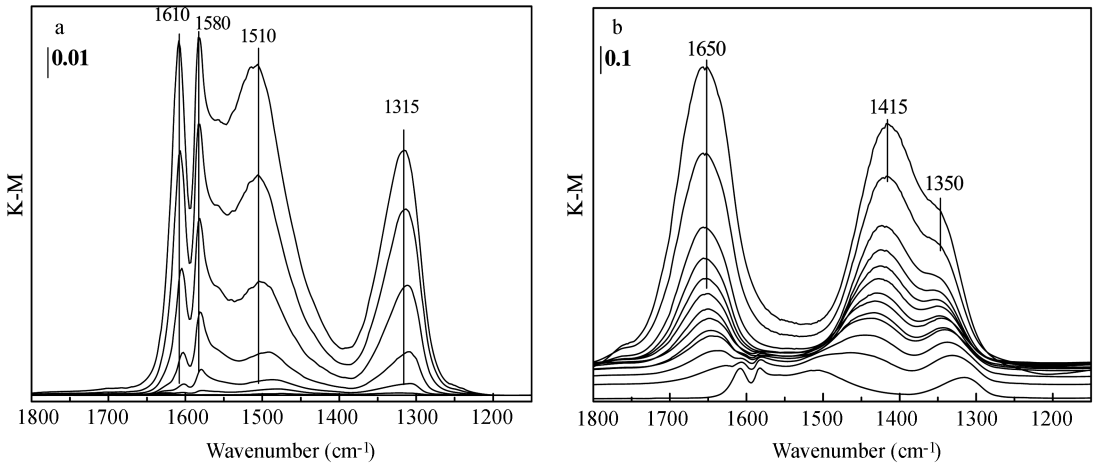

Fig. 7 DRIFTS spectra of TiO_2. (a) exposure of NO (200×10^{-6}, *V/V*) in simulated air (total flow: 100 mL/min, O_2: 21%) as a function of time; (b) exposed to water as a function of RH (%) (2.8, 6.5, 11.2, 15.4, 19.5, 24.1, 32.0, 41.1, 49.2, 58.1, 69.3, 81.2, 92.3) after nitrated at 30°C.

intensity to water adsorption layers. Figure 6 shows that about 1–5 layers of adsorbed water was present in the RH region 20%–90%. It was suggested that in ambient atmosphere, these mineral oxides always covered with several layers adsorbed water.

2.3 Water adsorption on nitrated oxides

The oxides were exposed to NO (200×10^{-6}, *V/V*) in the total flow 100 mL/min simulated air (79% N_2 + 21% O_2), and then the nitrated oxides were exposed to water after the introduction of NO and O_2 ceased. The DRIFTS spectra for TiO_2 are shown in Fig. 7, and several peaks at 1610, 1580, 1510 and 1315 cm^{-1} were observed as the exposure time increased (Fig. 7a). These peaks are assigned to bridging, monodentate, bidentate, and isolated nitrate (Underwood et al., 1999; Zhang et al., 2008). The mechanism of nitrate species formation on mineral oxides surfaces were studied thoroughly (Miller and Grassian, 1998; Underwood et al., 1999). Nitrite was observed as the intermediate which was then to form nitrate species by the reactions with gas-phase NO_2 in an Eley-Rideal type mechanism or with another surface nitrite in a Langmuir-Hinshelwood type mechanism (Underwood et al., 1999). NO, as a gas phase product of the transformation reaction, could be oxidized to NO_2 in the presence of excess O_2. After this process, the oxides surfaces were covered with nitrate species. When the RH increased from 2% to 95%, these peaks disappeared while the peak at 1650 cm^{-1} due to the bending mode of water as well as two peaks at 1415 and 1350 cm^{-1} which were due to water-solvated nitrate (Miller and Grassian, 1998; Goodman et al., 2001) were observed (Fig. 7b). Other oxides (expect SiO_2) exhibited the similar spectra (not shown here). It suggests that adsorbed water significantly affect the phase of surface nitrate species. On the other hand, the influences of the reaction with $NO+O_2$ on the hygroscopic behavior of oxides are also considered. The integration intensities of water absorption for nitrated oxides are also shown in Fig. 5. It shows clearly that the amounts of water adsorption were enhanced on the nitrated oxides compared to the fresh oxides. No deliquescence process for nitrate salts was observed. The reason may be that reaction of $NO+O_2$ on these oxides in a dry condition was only limited on the surface but not to the bulk of samples. However, these results of Fig. 5 indicated that atmospheric nitrated process has an important effect on the hygroscopic behavior of the mineral oxides. It is noteworthy that, because of the limited detection depth and therefore the saturation effect, infrared spectroscopy always provides qualitative and semi-quantitative information about the species analyzed. Therefore, the extent adsorbed water amount enhanced by nitrated reaction should be further measured through other methods.

3 Conclusions

In this study, *in situ* DRIFTS was used to study water adsorption on NaCl and mineral oxides. It demonstrates that DRIFTS is practical for studying the water adsorption on these samples. The DRH of NaCl measured by DRIFTS method is 74.2%, which is in good agreement with the reported data. For mineral oxides, all the water adsorption isotherms exhibited BET-III curve and the monolayers were formed at 24%–30% RH. About 1–5 layers of surface water were adsorbed at ambient relative humidity (20%–90% RH). Using this method, we found that nitrated process could enhance water adsorption amount significantly. Although *in situ* DRIFTS spectroscopy is an inexpensive and convenient method to study the adsorption processes on surface, the quantitative information should be further confirmed by other methods.

Acknowledgments

This work was supported by the National Natural Science Foundation of China (No. 20877084, 20937004) and the Chinese Academy of Sciences (No. KZCX2-YW-Q02-03).

References

Al-Abadleh H A, Grassian V H, 2003. FT-IR study of water adsorption on aluminum oxide surfaces. *Langmuir*, 19(2):

341–347.

Armaroli T, Becue T, Gautier S, 2004. Diffuse reflection infrared spectroscopy (DRIFTS): Application to the *in situ* analysis of catalysts. *Oil & Gas Science and Technology*, 59(2): 215–237.

Brunauer S, Deming L, Deming W, Teller E, 1940. On a theory of the van der Waals adsorption of gases. *Journal of the American Chemical Society*, 62(7): 1723–1732.

Brunauer S, Emmett P, Teller E, 1938. Adsorption of gases in multimolecular layers. *Journal of the American Chemical Society*, 60(2): 309–319.

Cziczo D J, Abbatt J P D, 2000. Infrared observations of the response of NaCl, $MgCl_2$, NH_4HSO_4, and NH_4NO_3 aerosols to changes in relative humidity from 298 to 238 K. *Journal of Physical Chemistry A*, 104: 2038–2047.

d'Almeida G, 1987. On the variability of desert aerosol radiative characteristics. *Journal of Geophysical Research–Atmospheres*, 92(3): 3017–3026.

Dentener F, Carmichael G, Zhang Y, Lelieveld J, Crutzen P, 1996. Role of mineral aerosol as a reactive surface in the global troposphere. *Journal of Geophysical Research-Atmospheres*, 101(D17): 22869–22889.

Fuller M, Griffiths P, 1978. Diffuse reflectance measurements by infrared Fourier transform spectrometry. *Analytical Chemistry*, 50(13): 1906–1910.

Goodman A L, Bernard E T, Grassian V H, 2001. Spectroscopic study of nitric acid and water adsorption on oxide particles: Enhanced nitric acid uptake kinetics in the presence of adsorbed water. *Journal of Physical Chemistry A*, 105(26): 6443–6457.

Gustafsson R J, Orlov A, Badger C L, Griffiths P T, Cox R A, Lambert R M, 2005. A comprehensive evaluation of water uptake on atmospherically relevant mineral surfaces: DRIFT spectroscopy, thermogravimetric analysis and aerosol growth measurements. *Atmospheric Chemistry and Physics*, 5(12): 3415–3421.

He H, Liu J F, Mu Y J, Yu Y B, Chen M X, 2005. Heterogeneous oxidation of carbonyl sulfide on atmospheric particles and alumina. *Environmental Science and Technology*, 39(24): 9637–9642.

IPCC (Intergovernmental Panel on Climate Change), 2007. Climate Change 2007: The Physical Science Basis. Contribution of Working Group I to the Fourth Assessment Report of the Intergovernmental Panel on Climate Change.

Krueger B J, Grassian V H, Iedema M J, Cowin J P, Laskin A, 2003. Probing heterogeneous chemistry of individual atmospheric particles using scanning electron microscopy and energy-dispersive X-ray analysis. *Analytic Chemistry*, 75(19): 5170–5179.

Liu Y C, Ma Q X, He H, 2009. Comparative study of the effect of water on the heterogeneous reactions of carbonyl sulfide on the surface of α-Al_2O_3 and MgO. *Atmospheric Chemistry and Physics*, 9: 6273–6286.

Miller T M, Grassian V H, 1998. Heterogeneous chemistry of NO_2 on mineral oxide particles: Spectroscopic evidence for oxide-coordinated and water-solvated surface nitrate. *Geophysical Research Letters*, 25(20): 3835–3838.

Tegen I, Fung I, 1994. Modeling of mineral dust in the atmosphere: Sources, transport, and optical thickness. *Journal of Geophysical Research-Atmospheres*, 99(D11): 22897–22914.

Underwood G M, Miller T M, Grassian V H, 1999. Transmission FT-IR and Knudsen cell study of the heterogeneous reactivity of gaseous nitrogen dioxide on mineral oxide particles. *Journal of Physical Chemistry A*, 103(31): 6184–6190.

Usher C R, Michel A E, Grassian V H, 2003. Reactions on mineral dust. *Chemical Review*, 103(12): 4883–4940.

Zhang X L, He H, Gao H W, Yu Y B, 2008. Experimental and theoretical studies of surface nitrate species on Ag/Al_2O_3 using DRIFTS and DFT. *Spectrochimica Acta Part A: Molecular and Biomolecular Spectroscopy*, 71(4): 1446–1451.

Zhang Y, Sunwoo Y, Kotamarthi V, Carmichael G, 1994. Photochemical oxidant processes in the presence of dust: An evaluation of the impact of dust on particulate nitrate and ozone formation. *Journal of Applied Meteorology*, 33(7): 813–824.